

Mechanism of Ground State Selection in the Frustrated Molecular Spin Cluster V_{15}

G. CHABOUSSANT^{1(*)}, S.T. OCHSENBEIN¹, A. SIEBER¹, H.-U. GÜDEL¹, H. MUTKA²,
A. MÜLLER³ and B. BARBARA⁴

¹ *Department of Chemistry, University of Berne, CH-3000 Bern 9, Switzerland.*

² *Institut Laue-Langevin, BP 156, 38042 Grenoble, France.*

³ *Department of Chemistry, University of Bielefeld, 33501 Bielefeld, Germany.*

⁴ *Laboratoire de Magnétisme Louis Néel, CNRS, BP 166, 38042 Grenoble, France.*

PACS. 75.30.Et – Exchange and superexchange interactions.

PACS. 75.50.Xx – Molecular magnets.

PACS. 78.70.Nx – Neutron inelastic scattering.

Abstract. – We report an inelastic neutron scattering (INS) study under a magnetic field on the frustrated molecular spin cluster V_{15} . Several field-dependent transitions are observed and provide a comprehensive understanding of the low-energy quantum spin states. The energy gap $2\Delta_0 \approx 27(3)\mu\text{eV}$ between the two lowest $S = 1/2$ Kramers doublets is unambiguously attributed to a symmetry lowering of the cluster. The INS data are mapped onto an $S=1/2$ Antiferromagnetic Heisenberg triangle with scalene distortion. A quantitative description of the wavefunction mixing within the ground state is derived.

Magnetic frustration operates when all the bonds in a magnetically coupled system cannot be satisfied simultaneously. The ground state is then best described by a superposition of quantum states with well defined probability of occurrence. However, small irregularities like lattice strains, structural disorder or quantum fluctuations can relieve part or all of the frustration, leading to a stabilised ground state with a gap to less favourable ground state configurations (*order by disorder* principle [1]). The field of frustrated magnetism is extremely active, encompassing low-dimensional materials [2,3], spin glasses or pyrochlores and Kagomé lattices [4]. Most of these materials are extended systems exhibiting short-range or quasi long-range order, a situation rarely encountered in molecular magnets (or spin clusters) where each such cluster in the lattice is magnetically well isolated from its neighbours due to the presence of surrounding ligands. This magnetic shielding allows the study of the individual behaviour of a finite number of interacting magnetic ions. Beside being ideal candidates to study fundamental processes like quantum tunnelling or quantum coherence at the nanoscale [5], molecular magnetic clusters, with their well defined nuclearities and topologies, also constitute quantum systems in which geometrical frustration effects at the molecular level can be addressed.

(*) Present address: Laboratoire Léon Brillouin (CNRS-CEA) CEA-Saclay, 91191 Gif-sur-Yvette Cedex, France. E-mail: chabouss@llb.saclay.cea.fr

A prominent example of a magnetically frustrated cluster is given by the polyoxovanadate complex $K_6[V_{15}^{IV}As_6O_{42}(D_2O)] \cdot 8D_2O$ (hereafter V_{15}) which contains 15 V^{4+} spins ($S = 1/2$) distributed over two hexagons capping one triangle with global spherical shape [6–8]. The clusters have D_3 symmetry without consideration of the hydrogen positions (inside and outside the cluster) and make up a molecular crystal with trigonal symmetry. The V^{4+} ions are antiferromagnetically (AFM) coupled to their neighbours via oxo-bridges. Within the hexagons, the AFM couplings are very strong (10-20 meV [9]) and the spins on the triangle are coupled to the spins of the hexagons via frustrated exchange couplings, but there are no significant *direct* exchange pathways between the triangle spins. The coupling between the triangle spins occurs *indirectly* through the hexagon spins. At low temperatures, the spins on the hexagons are quenched in a singlet ($S=0$) state, and we are left with the three triangle spins. The ground state is then made of two $S=1/2$ Kramers doublets separated from the $S=3/2$ quartet state by about 0.315 meV (3.7K) [10, 11]. Inelastic neutron scattering (INS) has shown that the two $S=1/2$ Kramers doublets are split by a gap $2\Delta_0 \approx 35\mu\text{eV}$ [10], and low-temperature magnetisation data were analysed in terms of a two-level Landau-Zener model with a gap of about $7 - 8\mu\text{eV}$ (80 – 100 mK) [11]. However, the microscopic origin of these gaps remained unclear. Recent theoretical work suggested that Dzyaloshinskii-Moriya (DM) interactions might be responsible for the gap opening [12].

In the present Letter, we report an INS study under a magnetic field of V_{15} and show that deviations from trigonal symmetry are responsible for the observed phenomena, not DM interactions. An analysis of both the energy levels and the Q -dependence enables us to characterise the distortion and to address the nature of the ground state.

The INS experiment was performed on the recently upgraded time-of-flight spectrometer IN5 at the Institut Laue-Langevin (ILL, France) using cold neutrons of wavelengths $\lambda = 7.5, 9$ and 11\AA . Data were collected at temperatures between 40mK and 50mK and corrected for the background and detector efficiency. The magnetic field was provided by a 2.5 Tesla superconducting coil. The instrumental resolution at the elastic line (Γ , Full-Width at Half-Maximum) is $\Gamma = 28\mu\text{eV}$ at 7.5\AA , $\Gamma = 18 - 21\mu\text{eV}$ at 9.0\AA and $\Gamma = 12\mu\text{eV}$ at 11\AA . We used a 4.6 g polycrystalline powder sample of fully deuterated V_{15} placed under Helium in a rectangular flat Aluminum slab.

Figure 1 shows INS spectra obtained at 7.5\AA and 9.0\AA for different values of the magnetic field. At $H=0\text{T}$, only one transition can be observed at an energy of ≈ 0.335 meV with $\Gamma \approx 41\mu\text{eV}$. This width is 1.5 broader than the instrumental resolution and is intrinsic [14]. As the field is switched on, satellite peaks appear *symmetrically* on each side of the main peak but with different intensities. At 1T, there is new intensity at about 0.12 meV. To better characterise it, the difference between the $H=0.5/1\text{T}$ and 0T data is shown in fig. 1c along with a higher resolution ($\lambda = 11\text{\AA}$) spectrum obtained at 0.65T. There are two peaks separated by about $\approx 25 - 30\mu\text{eV}$, and their energies increase linearly with magnetic field. Their widths are found to be between 17 and $19\mu\text{eV}$, in the range of the instrumental resolution, in contrast to the higher-energy peaks shown in fig. 1. Compiling the information derived from fig. 1, it is possible to draw the field-dependence of the INS transitions (see fig. 2a) where the five transitions are labeled (I) to (V).

To model our data, we consider the $S = 1/2$ Heisenberg Antiferromagnetic (HAFM) model on a triangle [7, 8]:

$$\mathcal{H}_0 = J_{12}\mathbf{S}_1\mathbf{S}_2 + J_{23}\mathbf{S}_2\mathbf{S}_3 + J_{13}\mathbf{S}_1\mathbf{S}_3 + \mathcal{H}_H, \quad (1)$$

where $\mathbf{S}_1, \mathbf{S}_2, \mathbf{S}_3$ denote the spin operators 1,2 and 3, respectively and J_{ij} is the Heisenberg exchange parameter between spins i and j . $\mathcal{H}_H = \mu_B\mathbf{H}(g_1\mathbf{S}_1 + g_2\mathbf{S}_2 + g_3\mathbf{S}_3)$ is the Zeeman interaction where the g_i -tensors are assumed to be diagonal. The Zeeman splitting of the

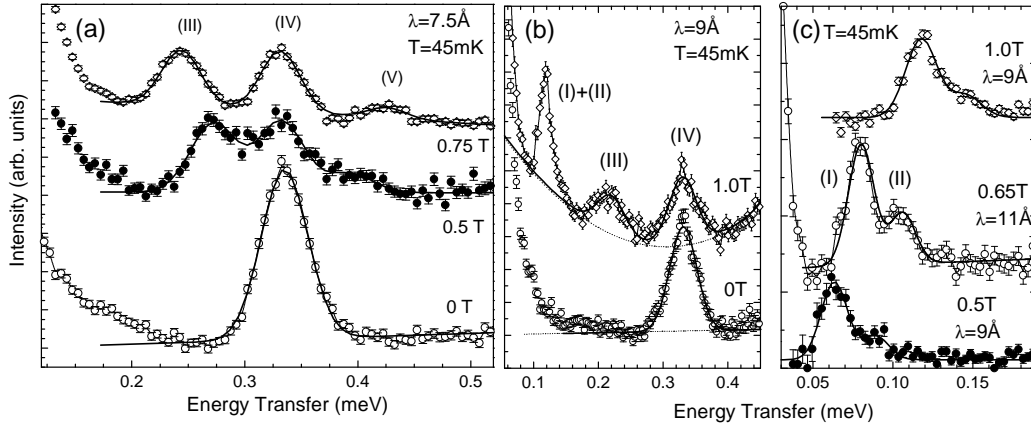


Fig. 1 – (a) INS spectra at 0, 0.5 and 0.75 T ($\lambda = 7.5\text{\AA}$). (b) INS spectra at 0 and 1.0 T ($\lambda = 9.0\text{\AA}$) (c) INS spectra at 0.65 T ($\lambda = 11.0\text{\AA}$) and difference plots between non-zero magnetic field ($H=0.5\text{ T}$, 1.0 T) and zero-field data obtained at $\lambda = 9.0\text{\AA}$. Data in the Q -range between 0.2\AA^{-1} and $1.1\text{--}1.4\text{\AA}^{-1}$ were grouped together to improve statistics. Solid lines are best fits to the data using Gaussian line shapes and a background. Peaks are labeled as discussed in the text.

energy levels does not depend on the relative orientation to the trigonal axis for isotropic couplings. For the equilateral HAFM triangle case ($J_{ij} = J_0 > 0$), the ground state consists of two degenerate $S=1/2$ Kramers doublets separated from the $S = 3/2$ excited state by $3J_0/2$. The wave functions of the two degenerate $S=1/2$ Kramers doublets are given by $\Psi_0^{\pm\frac{1}{2}} = |0, \frac{1}{2}, \pm\frac{1}{2}\rangle$ and $\Psi_1^{\pm\frac{1}{2}} = |1, \frac{1}{2}, \pm\frac{1}{2}\rangle$ in the basis $|S_{12}, S, M\rangle$ or any linear combination of them. If we assume inequivalent couplings, there is a gap $2\Delta_0$ between the two Kramers doublets but no splitting in the $S = 3/2$ state. For instance, in the isosceles case ($J_{12} = J$, $J_{13} = J_{23} = J'$) with $J > J'$, the energy gap becomes $2\Delta_0 = J - J'$ and $\Psi_0^{\pm\frac{1}{2}}$ is the lowest doublet.

From the field-dependence of the INS transitions shown in fig. 2a, we can immediately construct the energy diagram shown in fig. 2b corresponding to a distorted $S=1/2$ HAFM triangle with two $S=1/2$ doublet states and one $S=3/2$ quartet state. Note that at $T = 45$ mK, only the lowest doublet is populated in zero-field. Transitions (I) and (II) are intra-doublet transitions with energies $\hbar\omega_I = h = g\mu_B H$, $\hbar\omega_{II} = h + 2\Delta_0$, and transitions (III) to (V) are transitions from the lowest doublet to the $S=3/2$ sublevels with $\hbar\omega_{III} = 3J_0/2 + \Delta_0 - h$, $\hbar\omega_{IV} = 3J_0/2 + \Delta_0$ and $\hbar\omega_V = 3J_0/2 + \Delta_0 + h$. The transition $\hbar\omega = 2\Delta_0$ between the two doublets at zero-field could not be observed due to the width of the elastic line. The solid lines in fig. 2a corresponds to best fits with $g = 1.98(3)$, $2\Delta_0 = 27(3)\mu\text{eV} \approx 0.31(4)\text{K}$ and $J_0 = 212(2)\mu\text{eV} \approx 2.46\text{K}$. The g -factor value is in good agreement with EPR [7, 13] and millimeter range spectroscopy [15], the gap $2\Delta_0$ is in relatively good agreement with previous but less accurate INS measurements [10], and the value of J_0 is very close to the one inferred from magnetisation [11] and INS [10]. So far, the isosceles triangle scenario successfully explains the existing data, but there is no reason, *a priori*, to choose an isosceles triangle: Lattice distortions, being static or dynamic, will most probably generate a scalene triangle situation. From inspection of the energy levels it is not possible to discriminate between isosceles and scalene triangles. We demonstrate now that the INS intensities can discriminate between the two models.

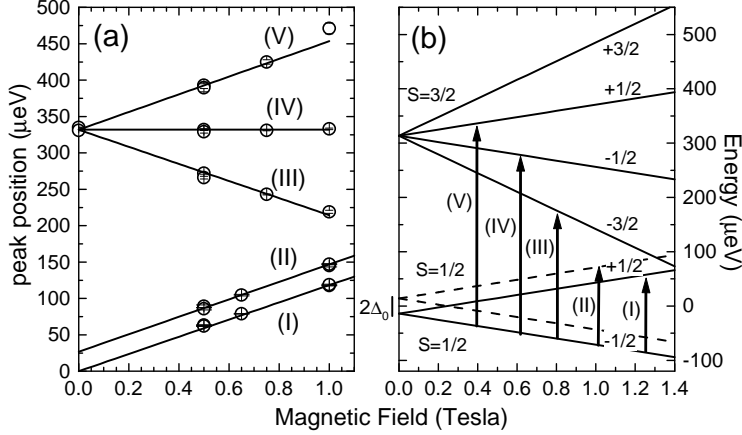


Fig. 2 – (a) Field-dependence energies of the observed INS peaks (I) to (V). Solid lines are linear fits to the data as discussed in the text. (b) Zeeman splittings and assignment of the observed INS transitions.

The differential magnetic cross-section for a transition between initial state $|S_{12}, S, M\rangle$ with energy E_s and final state $|S'_{12}, S', M'\rangle$ with energy E_f is given by [16]:

$$\frac{d^2\sigma}{d\Omega dE} = B_{\mathbf{Q}} \sum_{\alpha} \left(1 - \frac{Q_{\alpha}^2}{Q^2}\right) \sum_{i,j} e^{i\mathbf{Q}(\mathbf{R}_i - \mathbf{R}_j)} \quad (2)$$

$$\times \langle S_{12}, S, M | S_i^{\alpha} | S'_{12}, S', M' \rangle \langle S'_{12}, S', M' | S_j^{\alpha} | S_{12}, S, M \rangle \times \delta(\hbar\omega + E_s - E_f),$$

with

$$B_{\mathbf{Q}} = \frac{N e^{-\beta E_i} |\mathbf{k}'|}{Z |\mathbf{k}|} \cdot F^2(\mathbf{Q}) \cdot e^{-2W(\mathbf{Q})}. \quad (3)$$

N is the number of magnetic centres in the sample, \mathbf{k} and \mathbf{k}' are the initial and final neutron wave-vectors and $\mathbf{Q} = \mathbf{k} - \mathbf{k}'$ is the scattering vector, $\exp[-2W(\mathbf{Q})]$ is the Debye-Waller factor, $F(\mathbf{Q})$ is the magnetic form factor of the V^{4+} ions, \mathbf{R}_i is the position of the i th V^{4+} ion in the triangle, $\alpha = x, y$ or z , $\hbar\omega$ is the energy transfer and Z the partition function. The matrix elements $\langle S_{12}, S, M | S_i^{\alpha} | S'_{12}, S', M' \rangle$ are evaluated using irreducible tensor operator (ITO) methods [17]. Only the triangular model is considered. In the equilateral case, the *zero-field* and powder averaged cross-section for the transition $|S_{12}, S\rangle$ to $|S'_{12}, S'\rangle$ is [18]:

$$\frac{d^2\sigma}{d\Omega dE} \sim B_{\mathbf{Q}} \left(1 - \frac{\sin(QR)}{QR}\right) \mathcal{M}(S_{12}, S, S'_{12}, S'), \quad (4)$$

where R is the V^{4+} - V^{4+} separation in the triangle and \mathcal{M} is a number that depends on the initial and final state quantum numbers. One can show that it makes no difference to the INS intensities in zero magnetic field whether we have $S_{12} = 0$ or $S_{12} = 1$ in the lowest doublet. In order to compare the theoretical predictions with our experimental data, we need to consider the effect of the magnetic field. This is done by using the Wigner-Eckart theorem [18]. This leads to INS intensities depending explicitly on M, M' with selection rules $M - M' = 0, \pm 1$. We obtain the following intensity ratios for the doublet-quartet transitions (III:IV:V) = (3:2:1). The intra-doublet transition with $\Delta S_{12} = S_{12} - S'_{12} = \pm 1$ has the same

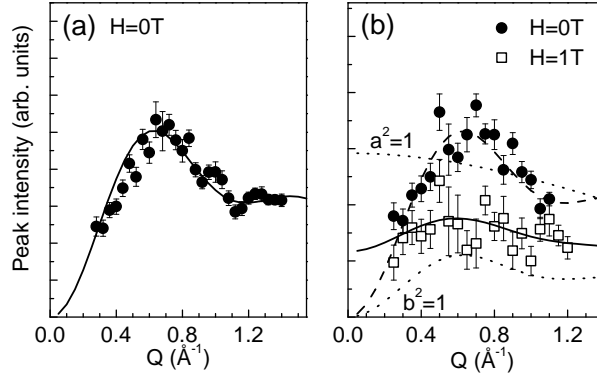


Fig. 3 – (a) Q -dependence of the transitions III + IV + V measured at zero-field, shown in fig. 1. (b) Q -dependence of transition (I) at 1T and $\lambda = 9\text{\AA}$ (open squares) along with the III+IV+V transitions measured at 0T and at the same wavelength. Lines (dashed and solid) are best fits using the calculated Q -dependence (eq. 4) and the $V - V$ distance $R = 6.92\text{\AA}$. Dotted lines correspond to theoretical curves with $a^2 = 1$ and $b^2 = 1$ (see text).

relative intensity as transition (IV), whereas the $\Delta S_{12} = 0$ transition is calculated to be three times more intense. Comparison with the data in fig. 1 shows good, but not perfect agreement for the doublet-quartet transitions, as (III) and (IV) have almost equal intensity, instead of the calculated ratio 3/2. From the relative intensity of the intra-doublet transitions we can tentatively assign transition (I) to have $\Delta S_{12} = 0$ and transition (II) to have $\Delta S_{12} = \pm 1$. We already note at this point, however, that transition (I) is weaker than the sum of (III), (IV) and (V).

To get further insight into the nature of the transitions, in particular the intra-doublet ones, we now consider their Q -dependence. Fig. 3a shows the Q -dependence of the sum of (III), (IV) and (V), measured at zero-field. The agreement with the Q -dependence calculated with Eq. 4 and the V - V distance $R = 6.92\text{\AA}$ is very good, a confirmation that the $S=3/2$ state is essentially unperturbed. Fig. 3b shows the same transitions, *i.e.* (III+IV+V) measured at zero-field and $\lambda = 9\text{\AA}$ (full circles), in comparison with the Q -dependence of transition (I) at 1T at the same wavelength (open squares) [19]. While the doublet to quartet transition shows the same Q -dependence as in fig. 3a, the intensity of (I) is much less Q -dependent, almost flat. Theoretically, an intra-doublet transition with $\Delta S_{12} = \pm 1$ would be modulated by the $[1 - \sin(QR)/QR]$ factor in eq. 4. On the other hand, a $\Delta S_{12} = 0$ transition does not have this factor and its Q -dependence is essentially flat. We have already tentatively assigned band (I) to a Zeeman transition within the same doublet ($\Delta S_{12} = 0$), and the Q -dependence now confirms this. However, we also note, and fig. 3b makes it very clear, that the overall intensity of peak (I) is significantly smaller than the sum of (III+IV+V). The pure $\Delta S_{12} = 0$ transition would have the same intensity, and the pure $\Delta S_{12} = \pm 1$ would be three times weaker. This clearly suggests that the two doublets Ψ_0^\pm and Ψ_1^\pm are mixed in V_{15} as expected for a scalene triangle. Defining the lower-lying doublet as $\Omega_0^\pm = a\Psi_0^\pm + b\Psi_1^\pm$ (with $a^2 + b^2 = 1$), we get the following Q -dependent intensity for transition (I):

$$I_I(Q) = I_0 F^2(Q) \left[a^2 + \frac{b^2}{3} \left(1 - \frac{\sin(QR)}{QR} \right) \right], \quad (5)$$

where I_0 is an intensity factor, kept fixed to the value determined from the intensity of (III+IV+V) at the same wavelength. The dotted lines in fig. 3b represent the disentangled

situations ($[a, b]=[1, 0]$ or $[0, 1]$) and the full line is a best fit to the data corresponding to $a^2 = 0.4$ and $b^2 = 0.6$. The mixing of the $S_{12} = 0$ and $S_{12} = 1$ states is quite substantial. One parameter set that produces this situation is $J_{12} = 0.21$ meV, $J_{23} = 0.23$ meV and $J_{13} = 0.20$ meV. This set is not unique as we only have access to a^2 and b^2 , but it gives a clear idea of the exchange coupling variation caused by the distortion.

We now briefly discuss the relevance of Dzyaloshinskii-Moriya (DM) interactions [12]. The effect of DM interactions in the S=1/2 AFM triangle has been treated in some detail [20] and we give here the main results. The DM interaction introduces off-diagonal matrix elements which lead to a first order splitting 2Δ of the doublets. If we assume perfect triangular symmetry, we have $2\Delta = d_z/\sqrt{3}$ [21] where d_z is the DM parameter. If the splitting in V_{15} was due to DM interactions this would lead to $d_z = 47\mu\text{eV}$. In contrast to the pure Heisenberg case, the energy levels depend explicitly on the relative orientation of the clusters to the magnetic field in this case [20]. In a powder measurement, the overall spectrum will reflect this field dependence by a broadening of all the peaks, in particular the intra-doublet transitions. This is clearly not what we observe experimentally. In addition, the theoretical energy difference 2Δ in the DM model between transitions (I) and (II) is field dependent, decreasing from $27\mu\text{eV}$ at 0T to $17\mu\text{eV}$ at 1T for a d_z value of $47\mu\text{eV}$. Again, this is completely incompatible with our experimental results, which show a field independent energy difference between (I) and (II) as well as a linear field dependence of transitions (III),(IV) and (V), see fig. 2. DM interactions can thus definitely be ruled out as the origin of the ground state splitting in V_{15} .

The present study demonstrates that the low-energy properties of V_{15} are accurately described by a triangle model with *scalene* distortion. In particular, the mechanism generating a gap $2\Delta_0 = 27(3)\mu\text{eV}$ between the two Kramers doublets is unambiguously established using both energy and wavefunction information provided by INS. The symmetry lowering is already established from the field dependence of the energy levels. However, *only* inspection of the intensities and their Q -dependence leads to a detailed knowledge of the wavefunction mixing within the ground state resulting from the scalene distortion of the triangle. An obvious source of symmetry lowering is provided by the water molecule located in the center of the spherical cavity of V_{15} . Another one is given by some disorder (partial occupancy) on the water structure of the lattice [7, 8, 22]. This study shows that the impact of very small structural perturbations to relieve magnetic frustration can be sizeable. V_{15} constitutes a example of a nanometer-scale system with maximised magnetic frustration (triangle) where *order, i.e.* a stabilised ground state with a gap to less favourable "ground states", is induced by a small structural distortion (*disorder*).

* * *

We are grateful to F. Mila and M. Elhajal for stimulating discussions, to J.-L. Ragazzoni and S. Jenkins for their technical support at the ILL and to E. Krickemeyer and H. Bögge for help in the synthesis. We wish to thank J. Ollivier, M. Plazanet and the IN5 team at the ILL for the very significant improvement of the spectrometer. One of us (A.M) thanks the Deutsche Forschungsgemeinschaft and the Fonds der Chemischen Industrie for financial support. This work has been supported by the Swiss National Science Foundation and by the TMR program Molnanomag of the European Union (No: HPRN-CT-1999-00012).

REFERENCES

- [1] VILLAIN J., *Z. Physik B*, **33** (1979) 31; VILLAIN J., BIDEAUX R., CARTON J.P and CONTE R., *J. Phys. (Paris)*, **41** (1980) 1263.

- [2] KODAMA K., TAKIGAWA M., HORVATIC M., BERTHIER C., KAGEYAMA H., UEDA Y., MIYAHARA S., BECCA F. and MILA F., *Science*, **298** (2002) 395 and references therein.
- [3] WESSEL S., NORMAND B., SIGRIST M. and HAAS S., *Phys. Rev. Lett.*, **86** (2001) 1086.
- [4] For a review see RAMIREZ A.P. in *Handbook on Magnetic Materials*, **13** (1999) 423 (Elsevier Science, Amsterdam); BRAMWELL S.T. and GINGRAS M.J.P., *Science*, **294** (2001) 1495; MOESSNER R., *Can. J. Phys.*, **79** (2001) 1283.
- [5] BARBARA B., THOMAS L., LIONTI F., CHIORESCU I. and Sulpice A., *J. Mag. Magn. Mat.*, **200** (1999) 167; SESSOLI R. and GATTESCHI D., *Angew. Chem. Int. Edit.*, **42** (2003) 268.
- [6] MÜLLER A. and DÖRING J., *Angew. Chem., Int. Ed. Engl.*, **27** (1988) 1721.
- [7] BARRA A. L., GATTESCHI D., PARDI L., MÜLLER A. and DÖRING J., *J. Am. Chem. Soc.*, **114** (1992) 8509.
- [8] GATTESCHI D., PARDI L., BARRA A. L. , MÜLLER A. and DÖRING J., *Nature*, **354** (1991) 463.
- [9] KOSTIYUCHENKO V.V and ZVEZDIN A.K., *Phys. Sol. State*, **45** (2003) 903;
PLATONOV V.V., TATSENKO O.M., PLIS V.I., POPOV A.I., ZVEZDIN A.K. and BARBARA B., *Phys. Stat. Sol.*, **44** (2002) 2104.
- [10] CHABOUSSANT G., BASLER R., SIEBER A., OCHSENBEIN S.T, DESMEDT A., LECHNER R.E., TELLING M. T. F., KÖGERLER P., MÜLLER A. and GÜDEL H.-U., *Europhys. Lett.*, **59** (2002) 291.
- [11] CHIORESCU I., WERNSDORFER W., MÜLLER A., BÖGGE H. and BARBARA B., *J. Mag. Mag. Mat.*, **221** (2000) 103; CHIORESCU I., WERNSDORFER W., MÜLLER A., BÖGGE H. and BARBARA B., *Phys. Rev. Lett.*, **85** (2000) 3454; CHIORESCU I., WERNSDORFER W., MÜLLER A., MIYASHITA S. and BARBARA B., *Phys. Rev. B*, **67** (2003) 020402.
- [12] KONSTANTINIDIS N.P. and COFFEY D., *Phys. Rev. B*, **66** (2002) 174426; DE RAEDT H., MIYASHITA S. and MICHIELSEN K., cond-mat 0306275.
- [13] AJIRO Y. ITOH H., INAGAKI Y., ASANO T., NARUMI Y., KINDO K., SAKON T., MOTOKAWA M., CORNIA A., GATTESCHI D., MÜLLER A. and BARBARA B., in Proceedings of French-Japanese Symposium at Fukuoka , Japan (2001).
- [14] At $\lambda = 9.0\text{\AA}$, the resolution is better and, at zero-field, the width of the main line is still around $40\mu\text{eV}$. Therefore the intrinsic width of the 0.335 meV peak is $40\mu\text{eV}$.
- [15] VONGTRAGOOL S., GORSHUNOV B., MUKHIN A.A., VAN SLAGEREN J., DRESSEL M. and MÜLLER A., *Phys. Chem. Chem. Phys.*, **5** (2003) 2778.
- [16] LOVESEY S.M., Theory of Thermal Neutron Scattering from Condensed Matter, (Clarendon Press Oxford), 1984.
- [17] BUDD B.R., Operator Techniques in Atomic Spectroscopy (McGraw-Hill, New-York, 1963).
- [18] FURRER A. and GÜDEL H.-U., *Phys. Rev. Lett.*, **39** (1977) 657; FURRER A. and GÜDEL H.-U., *J. Mag. Mag. Mat.*, **14** (1979) 256.
- [19] At $\lambda = 7.5\text{\AA}$ transition (I) is in the tail of the elastic line and it is not possible to obtain a reliable Q -dependence of this transition with this setting. Thus, to compare its Q -dependence with the main transition at zero-field, we consider the $\lambda = 9.0\text{\AA}$ data where the two transitions are observed under the same conditions.
- [20] TSUKERBLAT B.S., KUYAVSKAYA B.Y., BELINSKII M.I., ABLOV A.V., NOVOTORTSEV V.M. and KALINNIKOV V.T., *Theoret. Chim. Acta (Berl.)*, **38** (1975) 131; RAKITIN Y.V., YABLOKOV Y.V. and ZELENTSOV V.V., *J. Magn. Res.*, **43** (1981) 288.
- [21] BOČA R., Theoretical Foundations of Molecular Magnetism, Elsevier (1999).
- [22] CHOI J., SANDERSON L.A.W., MUSFELDT J.L., ELLERN A., and KÖGERLER P., *Phys. Rev. B.*, **68** (2003) 064412.